Materials Science

AIMS Materials Science, 7(1): 24–32.
DOI: 10.3934/matersci.2020.1.24
Received: 08 October 2019
Accepted: 25 November 2019
Published: 13 January 2020

http://www.aimspress.com/journal/Materials

Research article

Fluxless ultrasonic soldering of SiC ceramics and Cu by Bi–Ag–Ti based solder

Daniela Šuryová*, Igor Kostolný and Roman Koleňák

Faculty of Materials Science and Technology in Trnava, Slovak, University of Technology in Bratislava, Jána Bottu No. 2781/25, 917 24 Trnava, Slovak Republic

* **Correspondence:** Email: daniela.suryova@stuba.sk.

Abstract: The aim of this research was to study the microstructure in soldered joint of SiC ceramics with Cu in cases of flux-less soldering with ultrasound assistance. The soldering was performed by ultrasonic activation of newly developed Bi–Ag–Ti based solder alloy. This new solder alloy was developed for flux-less soldering processes and meets the requirements for the versatility of its use for soldering metal and ceramic materials.

Suitability for the application of Bi–Ag–Ti solder was assessed on the basis of analyses of joint boundaries and measuring the shear strength of the joint. Light analysis proved the formation of joints without cracks, pores or other imperfections. The SiC/Bi–Ag–Ti boundary was formed on the basis of the reaction between Si and Ti. The bond in Cu/Bi–Ag–Ti boundary was formed due to formation of mechanical mixture of Bi + Cu. The average shear strength of the SiC/Cu joint reached 40 MPa.

Keywords: soldering; SiC ceramic; ultrasonic soldering; Bi solder; Cu substrate; microstructure

1. Introduction

SiC ceramics are often used in electronic devices as a semiconductor component in the manufacture of MOSFET (Metal Oxide Semiconductor Field Effect Transistor), IGBT (Insulated Gate Bipolar Transistor), DMOS (Double diffused Metal Oxid Semiconductor), SiC–DMOS (Silicon Carbid Double diffused Metal Oxid Semiconductor), SiC–SBD (Silicon Carbid transistors0 and other components [1,2]. The semiconductor is usually connected to THE conductive part of a packaged unit [3].

Soldering is the most used technology employed for bond formations between SiC semiconductors and conductive parts. Great attention is at present devoted to soldering with ultrasound assistance without the use of flux [4–8]. Many authors at present deal with the issues of soldering SiC ceramics with Cu [9–11].

A group of scientists [12] has dealt with the research of a suitable solder for applications at higher service temperatures in the automotive industry. They solved the application of a power SiC device in electronic hybrid vehicles with a service temperature around 200 °C. The capability to operate SiC-based power electronic modules at higher temperatures significantly simplifies the control system, which in turn reduces total costs. Most of the lead-free, Sn or Bi-based solders exert a melting point within the temperature range of 170–229 °C, although these are not suitable for permanent service at higher application temperatures. Therefore the BiAgPd and BiAgSn (AgBiX®, Indium Corporation) solders were developed as an alternative to a fluxless solder with a melting point of 265 °C [13–15]. This solder was developed with the aim to improve wettability, which enables a more intense formation of intermetallic phases in the joint boundary.

An alternative is solder with a matrix containing Ag particles [16–18]. This solder, which is destined for higher application temperatures, is often used for reactive soldering of SiC with aluminium oxide [19,20]. However, this effort is focused on the development of new universal solders that can join metal and ceramic materials in a direct way (without coatings or interlayers) by a flux-less method. The design of new solder alloys must also be based on the use of lead-free filler materials.

In this paper, research is directed to the use of a new solder alloy for higher application temperatures based on Bi–Ag–Ti. The solder was used to solder the SiC semiconductor substrate with Cu. This combination is directly focused upon power semiconductor applications. In this paper, the suitability of this alloy for soldering of this combination was evaluated on the basis of standard research methods. The joint microstructure and analyses of interactions on the boundary were studied and the shear strength of the joint was measured.

2. Materials and methods

Ultrasonic soldering was employed for soldering SiC ceramics with Cu. The CERAN 500 hot plate with thermostatic control was used as the heat source for melting solder. Surface oxides were removed by application of Hanuz UZP 2 ultrasonic equipment at a frequency of 40 kHz. Ultrasonic vibrations were applied for 3 to 5 s. The parameters of ultrasonic soldering are given in Table 1.

Table 1. Soldering parameters.

Parameters	
Ultrasound power	400 W
Working frequency	40 kHz
Amplitude	2 μm
Soldering temperature	380 °C
Time of ultrasound activation	5 s

Substrates of the following dimensions were used for soldering:

- SiC ceramics in the form of a disc in diameter of Φ 15 mm × 3 mm
- Copper in the form of a square in dimension of 10 × 10 × 2 mm

An active Bi–Ag–Ti-based solder was applied for joint fabrication. The chemical composition of the soldering alloy is given in Table 2.

Table 2. Chemical composition of soldering alloy.

Element	Quantity (hm%)
Bi	86
Ag	11
Ti	3

Figure 1 shows a schematic procedure of ultrasonic soldering. The melting temperature of the soldering alloy was measured by DTA analysis. The microstructure of the soldered joint was observed by use of light microscopy on NEOPHOT 32 equipment. The microstructure of joints was analysed by electron scanning microscopy (SEM). EDX analysis was applied for analysis of SiC/Bi11Ag3Ti and Cu/Bi11Ag3Ti joint boundaries. A LabTest 5.250SP1-VM device was used for shear strength measurement. A jig with a defined specimen shape was used to change the direction of application of the tensile axial loading force on the specimen. This special jig provides uniform shear loading to the specimen in the plane of the interface of the solder and substrate.

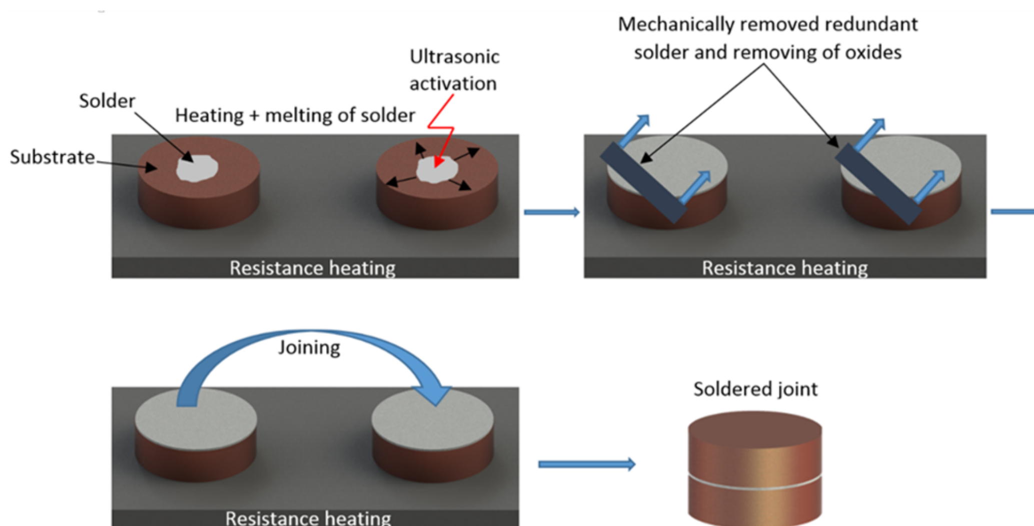

Figure 1. Shows a schematic procedure of ultrasonic soldering.

3. Results and discussion

Figure 2 shows the result of DTA analysis of soldering alloy type Bi11Ag3Ti. The analysis follows the course of solder heating from room temperature to melting point. The first reaction took place at a temperature of 258 °C. This temperature characterizes the eutectic transformation between Bi and Ag. It is the temperature at which the binary mixture of Bi–Ag begins to melt. The second reaction has occurred at a temperature of 366 °C, which is when total fusion of Bi–Ag mixture occurs. The third reaction took place at 399 °C. This reaction characterizes the fusion of the last phase of Ag–Ti. The melting point of Bi11Ag3Ti solder is 411 °C. Based on DTA analysis, the soldering temperature was determined to be 380 °C.

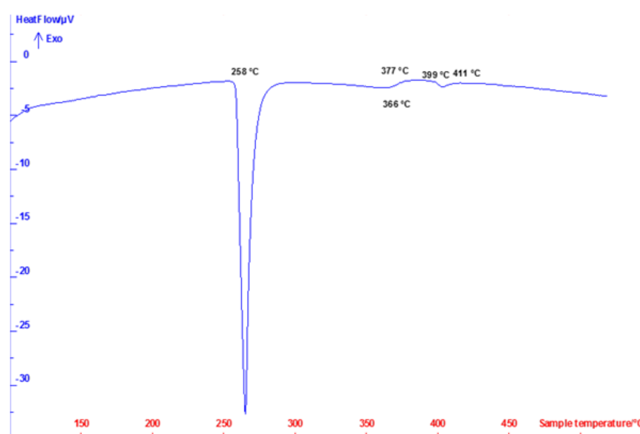

Figure 2. DTA analysis of soldering alloy type Bi11Ag3Ti.

Figure 3 shows the microstructure of the SiC/Bi11Ag3Ti/Cu soldered joint. The lower part of the joint is formed of Cu and the upper part consists of SiC. It is obvious from the figure that the bond is sound and free from cracks or pores. An undulated boundary may be seen between the solder and copper, which is caused by the effect of ultrasonic vibrations. The results of light microscopy suggest the presence Ti phases, which are concentrated not only in solder volume but also on the boundary with the copper substrate.

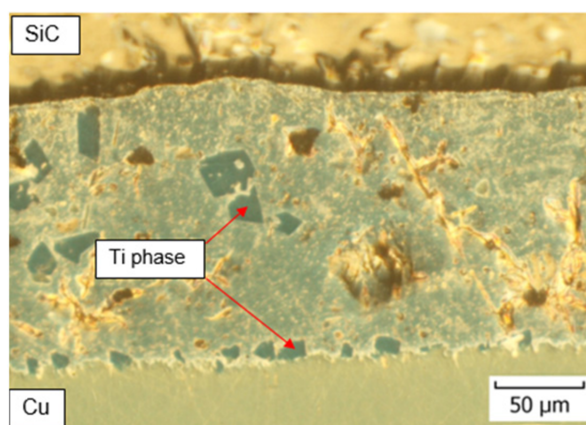

Figure 3. Microstructure of SiC/Bi11Ag3Ti/Cu joint.

EDX microanalysis was applied for the identification of constituents and phases. Figure 4 shows the results of line EDX microanalysis of the SiC/Bi11Ag3Ti joint.

The close boundary of the SiC/Bi11Ag3Ti joint was mainly formed of Bi and Ti. The minor presence of Ag was also proven. The bond was formed owing to an increased concentration of Ti, which is obvious from Figure 4—the green curve. Ti is an active component of solder. The high affinity of Ti to elements of the ceramics component ensured the reaction between Ti and ceramics at the formation of a reaction band. Based on line analysis, the diffusion of Si to the volume of soldering alloy was identified.

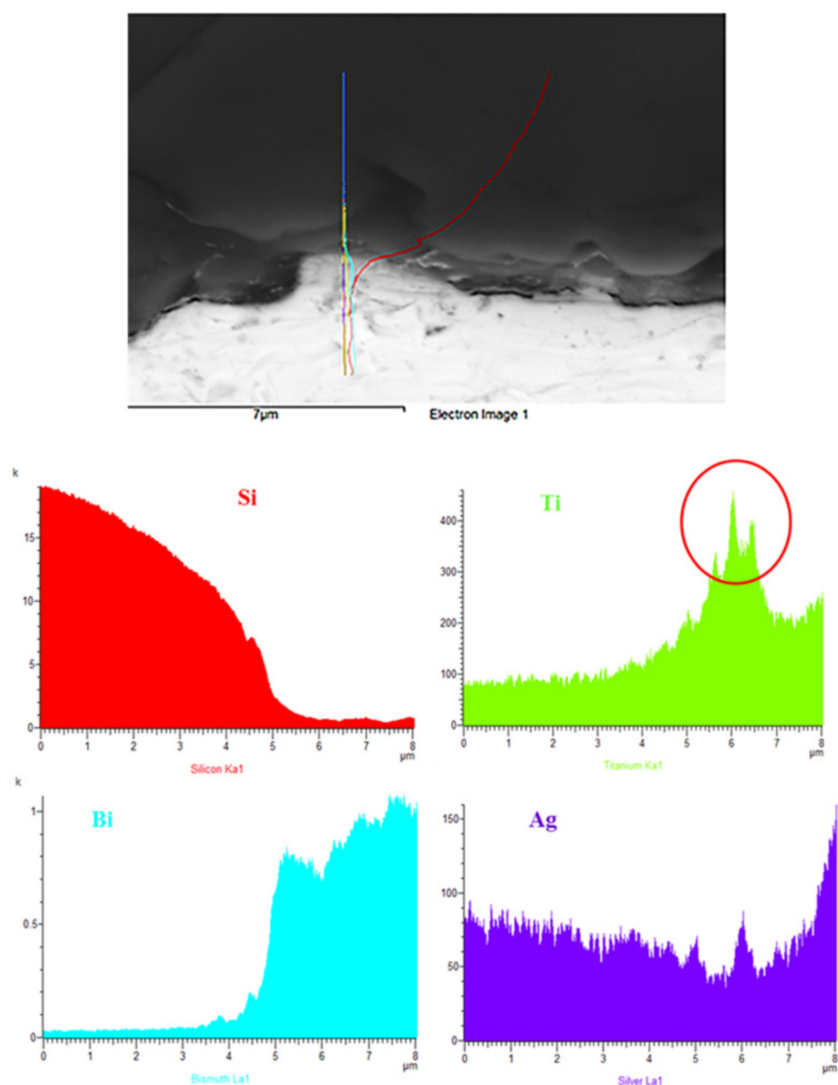

Figure 4. The line EDX microanalysis of boundary of SiC/Bi11Ag3Ti joint.

The diffused silicon is concentrated in the bond zone. Thus the reaction band is formed of the Ti–Si phase. The thickness of the reaction band at the point of measurement is approximately 1 µm. Figure 5 shows the map of elements in the boundary of SiC/Bi11Ag3Ti joint. The yellow color identifies the presence of Ti in the boundary. As is obvious from Figure 5, Ti was distributed to the boundary with SiC during the soldering process.

The planar distribution of elements also proved the presence of Si in the boundary. The presence of Si in the boundary is depicted in Figure 5 by green color. In several sections of the joint the presence of silver was also identified in the boundary—Figure 5d. Silver occurs in the solder in the form of an intermetallic phase.

Another analyzed boundary comprised the Cu/Bi11Ag3Ti joint. The EDX line analysis was performed in this boundary and its results are shown in Figure 6. No metallurgical bond was formed in the boundary between Cu and Bi11Ag3Ti solder. This finding was also proved by the authors in works [21,22]. Based on their observation, only a mechanical bond exists in the boundary. The presence of Ag and/or Ti was not identified in this boundary. Based on the line analysis it may be stated that the bond in a close boundary is formed by the mechanical mixture of Cu and Bi. The

thickness of the reaction band in Bi11Ag3Ti/Cu joint was approximately 0.8 μm.

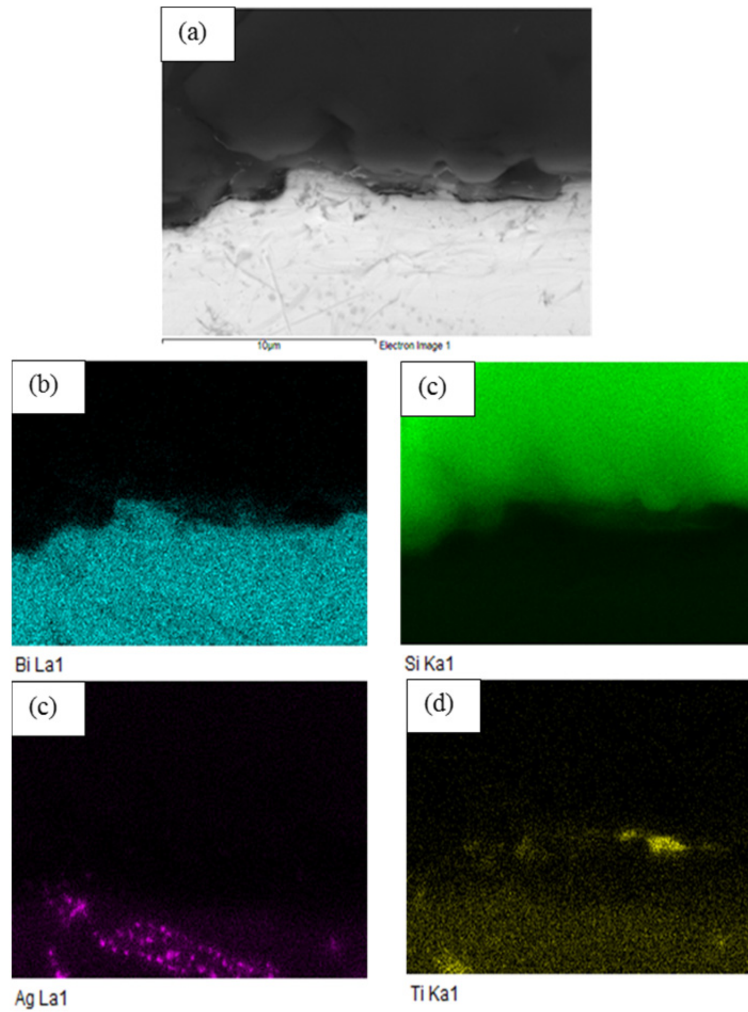

Figure 5. (a) Planar distribution of elements in the boundary of SiC/Bi11Ag3Ti joint (b) Si, (c) Bi, (d) Ag, and (e) Ti.

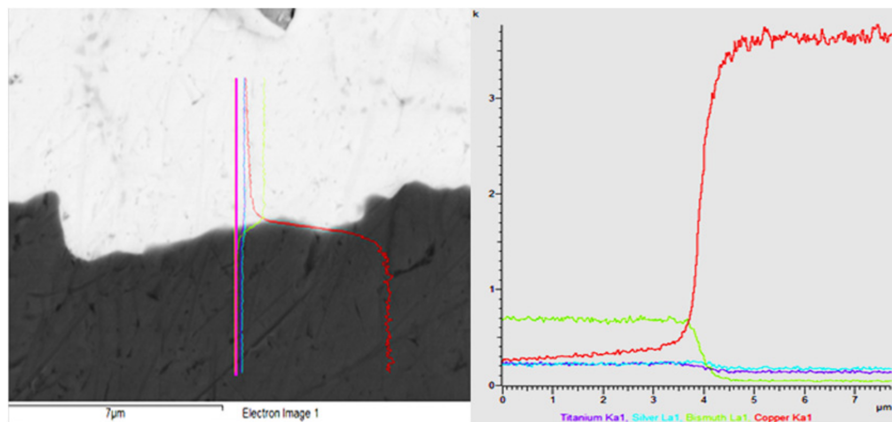

Figure 6. Line EDX microanalysis in the boundary of Cu/Bi11Ag3Ti joint.

Finally, the shear strength of the joints soldered with Bi–Ag–Ti solder was measured. The shear strength was graphically evaluated and is shown in Figure 7. An important value for this work was the result of the average shear strength of the SiC/Cu joint, which is marked in red in the graph. The average value reached 40 MPa.

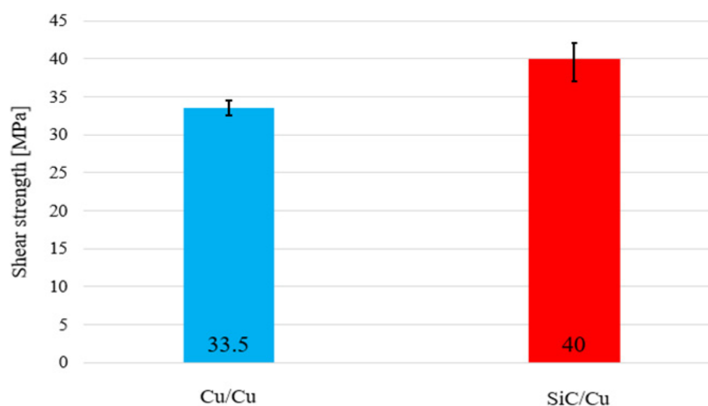

Figure 7. Shear strength of the joints soldered with Bi–Ag–Ti solder.

For comparison, shear strength was also measured at the Cu/Cu joint. The average strength of this joint was 33.5 MPa. The SiC/Cu combination is a main combination for a large number of applications in modern electronics. In this study, this bond achieved a higher strength than the bond strength of metallic (Cu/Cu) substrates. The bond strength for applications in power semiconductor devices must be at least 40 MPa. A new solder alloy fulfills this condition.

4. Conclusion

The aim of this study was to assess the suitability of a newly developed active solder type Bi–Ag–Ti for soldering the SiC/Cu combination. This Bi–Ag–Ti based solder belongs to solders for higher application temperatures. Its selection is oriented for application in power semiconductor devices. The achieved results may be characterised as follows:

-The melting temperature of Bi11Ag3Ti solder and reactions during heating was determined on the basis of DTA analysis. Three reactions were observed. First reaction occurs at the temperature of 258 °C, when the binary mixture of Bi–Ag begins to melt. A second reaction at 366 °C represents the end of melting of Bi–Ag mixture. The third reaction—melting of Ag–Ti phase, occurs at 399 °C. The solder was completely melted at 411 °C.

-The microstructure of soldered joints was free from cracks, pores or other imperfections,

-The boundary in SiC/Bi11Ag3Ti joint was predominantly formed of Si–Ti based phase. The thickness of the reaction layer in the boundary was approximately 1 μm. The presence of an active element Ti ensured the wetting of SiC substrate during soldering process,

-The bond in the boundary of Bi11Ag3Ti/Cu joint was formed on the basis of formation of a mechanical mixture of Bi + Cu. The thickness of reaction layer in the boundary of SiC/Bi11Ag3Ti joint was approximately 0.8 μm. Titanium at the interface was not observed,

-The average shear strength of SiC/Cu joint was 40 MPa. This value was higher than the shear strength of the Cu/Cu joint (33.5 MPa).

The research of soldering the combination of SiC/Cu by use of Bi11Ag3Ti solder proved the suitability of application of the selected soldering alloy. Regarding the results of analyses of joint boundaries, the formation of a sound joint was proved. The average shear strength of SiC/Cu joint reached 40 MPa. This joint was even stronger than the Cu/Cu joint using the same solder. This value (40 MPa) of shear strength is suitable for applications in modern power semiconductor devices.

Acknowledgments

This work was supported by the Slovak Research and Development Agency under the contract no. APVV-17-0025. The paper was also prepared with the support of the VEGA 1/0089/17 project: Research of new alloys for direct soldering of metallic and ceramic materials and project for supporting excellent teams of young researchers in conditions of Slovak Technical University-Project Young Researcher-excellent teams-no. 1392.

Conflict of interests

All authors declare no conflicts of interest in this paper.

References

1. Rashid MH (2011) Power electronics devices, 3rd Eds., *Power Electronics Handbook*, Oxford: Butterworth–Heinemann, 1409.
2. Wintrich A, Nicolai U, Tursky W, et al. (2015) *Application Manual Power Semiconductors*, Germany: ISLE Verlag.
3. Bukhari MZ, Brabazon D, Hashmi MSJ (2011) Application of metal matrix composite of CuSiC and AlSiC as electronics packaging materials. *The 28th International Manufacturing Conference*.
4. Li MY, Wang CQ, Bang HS, et al. (2004) Development of a flux-less soldering method by ultrasonic modulated laser. *J Mater Process Tech* 168: 303–307.
5. Sung KK, Sarkhel AK (1994) Lead (Pb)-free solders for electronic packaging. *J Electron Mater* 23: 701–707.
6. Park JH, Kim TW, Zhang S, et al. (2016) Effects of polymer ball size and polyvinylidene fluoride nanofiber on the ball capture rate for 100-μm-pitch flex-on-flex assembly using anisotropic conductive films and ultrasonic bonding method. *IEEE T Comp Pack Man* 6: 1127–1134.
7. Shi Y, Fang W, Xia Z, et al. (2010) Investigation of rare earth-doped BiAg high-temperature solders. *J MaterSci-Mater El* 21: 875–881.
8. Hu FQ, Zhang QK, Jiang JJ, et al. (2018) Influences of Ag addition to Sn-58Bi solder on SnBi/Cu interfacial reaction. *Mater Lett* 214: 142–145.
9. Olesinska W, Pawłowska M, Kalinski D, et al. (2004) Reactive metallic layers produced on AIN, Si_3N_4 and SiC ceramics. *J Mater Sci-Mater El* 15: 813–817.
10. Luo H, Reigosa PD, Lannuzzo F, et al. (2018) On-line solder layer degradation measurement for SiC-MOSFET modules under accelerated power cycling condition. *Microelectron Reliab* 88–90: 563–567.

11. Akbarpoura MR, Mirabada HM, Alipour S (2019) Microstructural and mechanical characteristics of hybrid SiC/Cu composites with nano- and micro-sized SiC particles. *Ceram Int* 45: 3276–3283.
12. Shen ZZ, Fang K, Johnson RW (2014) Characterization of Bi–Ag–X solder for high temperature SiC die attach. *IEEE Tran Comp Pack Man* 4: 1778–1784.
13. Manikam VR, Paing S, Ang A (2013) Effects of soft solder materials and die attach process parameters on large power semiconductor dies joint reliability. *IEEE 15th Electronics Packaging Technology Conference (EPTC 2013)* 152–155.
14. Ge D, Che FX, Tay YS, et al. (2012) Study on creep fatigue behaviour of soft solders die attach for power package applications. *IEEE 14th Electronics Packaging Technology Conference (EPTC 2012)* 77–83.
15. Harkai E, Balogh B (2009) Investigation of die attach quality in power electronic devices. *32nd International Spring Seminar on Electronics Technology* 1–5.
16. Chen G, Cao Y, Mei Y, et al. (2012) Pressure-assisted low-temperature sintering of nanosilver paste for 5 × 5-mm^2 chip attachment. *IEEE Tran Comp Pack Man* 2: 1759–1767.
17. Xiao K, Calata JN, Zheng H, et al. (2013) Simplification of the nanosilver sintering process for large-area semiconductor chip bonding: reduction of hot-pressing temperature below 200 °C. *IEEE Tran Comp Pack Man* 3: 1271–1278.
18. Zheng H, Berry D, Calata JN et al. (2013) Low-pressure joining of large-area devices on copper using nanosilver paste. *IEEE Tran Comp Pack Man* 3: 915–922.
19. Zhang HW, Lee NC (2012) A drop-in die-attach solution for the high temperature lead-free BiAgX solder paste system. *IMPAS* 2012: 000058–000065.
20. Shen Z, Fang K, Hamilton M, et al. (2013) Lead-free solder attach for 200 °C applications. *IMPAS* 2013: 000260–000267.
21. Kim YS, Zhang S, Paik KW (2015) Highly reliable solder ACFs FOB (flex-on-board) interconnection using ultrasonic bonding. *J Microelectron Packag Soc* 22: 35–41.
22. Zhang S, Kim SH, Kim TW, et al. (2014) A study on the solder ball size and content effects of solder ACFs for flex-on-board assembly applications using ultrasonic bonding. *IEEE Tran Comp Pack Man* 5: 9–14.

AIMS Press

© 2020 the Author(s), licensee AIMS Press. This is an open access article distributed under the terms of the Creative Commons Attribution License (http://creativecommons.org/licenses/by/4.0)